Detailed Energy Model of the NIST Net-Zero Energy Residential Test Facility: Development, Modification, and Validation

ELIZABETH BALKE[1], GREGORY NELLIS[1], SANFORD KLEIN[1], HARRISON SKYE[2]*, VANCE PAYNE[2], TANIA ULLAH[2]
[1]*Solar Energy Laboratory, University of Wisconsin – Madison, Madison, WI, USA*
[2]*Engineering Laboratory, National Institute of Standards and Technology, Gaithersburg, MD, USA*

The NIST Net-Zero Energy Residential Test Facility (NZERTF) is a highly instrumented, highly configurable, single-family, net-zero energy house occupied by a virtual family of four. A detailed transient model of the NZERTF and the accompanying mechanical equipment was created using information available before construction; the model incorporated building geometric details and construction material properties, as well as manufacturers' specifications for HVAC, water heating, solar PV and other equipment. This model represents the typical design paradigm, where actual building performance and detailed equipment operation are not known. This original model underpredicted the measured annual energy consumption by 13.8 %.

The measured data were used to understand and correct the sources of error at the component level; modifications to the HVAC system, interior thermal capacitance, and domestic hot water system improved the energy consumption prediction to within 1.6 % of measured data. The differences between the original and modified models are useful for understanding the sources, magnitudes, and possible corrections to errors in energy models for high-efficiency residences. The modified model will be used in future studies of alternative energy system configurations and control strategies, contributing to cost-effective and optimum design of net-zero energy houses in America.

Elizabeth Balke** is an energy consultant. **Gregory Nellis** is a professor. **Sanford Klein** is an emeritus professor. **Harrison Skye, **Vance Payne**, and **Tania Ullah** are research engineers.*
**Corresponding author e-mail: harrison.skye@nist.gov*

Abbreviations

ASHRAE	American Society of Heating, Refrigeration, and Air-conditioning Engineers
CAD	computer aided design
CONTAM	a multi-zone indoor air quality and ventilation analysis computer program
DHW	domestic hot water
HPWH	heat pump water heater
HRV	heat recovery ventilator
HVAC	heating, ventilation, and air-conditioning
NIST	National Institute of Standards and Technology
NZERTF	net-zero energy residential test facility located on the NIST campus
PV	photovoltaic
SHW	solar hot water system

1 Introduction

The Net-Zero Energy Residential Test Facility (NZERTF) is a single-family house built at the National Institute of Standards and Technology (NIST) on its campus in Gaithersburg, Maryland. A net-zero energy building is defined here as a building that produces at least as much energy as it uses in a year when considered at the site (Torcellini et al. 2006). The NZERTF was built with two purposes: (1) to demonstrate that it is possible to achieve net-zero energy operation with a home that is similar in size and appearance to a typical Maryland house and (2) to evaluate various energy system configurations and control strategies in this context (Omar and Bushby 2013). The NZERTF contains an assortment of commercially-available building energy technologies, including three separate ground source heat exchangers, an air-to-air heat pump, a heat recovery ventilation system (HRV), a radiant basement floor heating system, a solar hot water system (SHW) with two differently-sized storage tanks, a heat pump water heater (HPWH), and a solar photovoltaic (PV) system. Only a subset of the available technology was used during the first year of operation, which ran from July 2013 to June 2014. Although the house is unoccupied, the activities associated with a family of four are simulated by activating appliances, plug loads, lighting, water draws, and devices that generate sensible and latent heat loads. These loads are activated per a weekly schedule specified in

Omar and Bushby (2013), which is based on standard user profiles developed for the Building America program operated by the U.S. Department of Energy (Hendron and Engebrecht 2010). During the first year of operation, the NZERTF exceeded the net-zero energy goal by generating 484 kWh more electricity than it consumed.

An accurate simulation model of the NIST NZERTF is necessary to carry out studies of various energy system configurations and control strategies in a net-zero house. An original detailed model of the NZERTF and the accompanying mechanical equipment have been created using a transient system simulation program (TRNSYS 17 2013); a more detailed discussion of the model is available in (Balke 2015). The building construction parameters used in original building model were determined or estimated from construction drawings and ASHRAE standard 90.2 (2007). The infiltration was estimated using the Sherman-Grimsrud model as presented in the Ventilation and Infiltration chapter of the ASHAE Handbook of Fundamentals (ASHRAE, 2017 and Sherman and Grimsrud, 1980). Soil temperatures were determined using (NRCS, 2017). Equipment specifications from manufacturer datasheets were used to develop subsystem models. Finally, The weather data was measured at a local airport 6.4 km from NIST campus (Montgomery County Airpark, KGAI, from July 1, 2013 to June 30, 2014).

Although the NZERTF is a well-documented and carefully monitored and controlled facility (Davis et al. 2014), creating an accurate detailed model was challenging. The original model provided estimates of the thermal loads and the electricity consumption of the subsystems within the house that were about 13.8 % different from measurements. The measured annual energy data were used to understand and correct the sources of error at the component level; modifications to the HVAC system, interior thermal capacitance, and domestic hot water system (DHW) improved the energy consumption prediction to within 1.6 % of measured data. The differences between the original and modified models are useful for understanding the sources, magnitudes, and possible corrections for errors in energy models for high-efficiency residences. The modified model will be used in future studies of alternative energy system configurations and control strategies, contributing to cost-effective and optimum design of net-zero energy houses in America.

2 Methods

2.1 Building Envelope Model

House Structure

The NZERTF is a two-story house with 251 m^2 (2702 ft^2) of living space and a 135 m^2 (1453 ft^2) conditioned basement. The NZERTF CAD model, shown in Figure 1, was created using the as-built architectural plans. An in-built Type 56 in the transient system simulation program was used to model the building, and the layers of material used in the walls, roof, floors, and ceilings were specified in accordance with the plans (Building America Corporation 2009; Leyde 2014). The model is divided into four zones: the basement (Zone 1), the main/first floor (Zone 2), the second floor (Zone 3), and the attic (Zone 4). Each zone is assumed to have a uniform temperature and humidity. Further details on the modeling of the building envelope are presented in Leyde (2014) and Balke (2015).

Infiltration

The infiltration model, Type 932, implements the Sherman-Grimsrud infiltration model (Sherman and Grimsrud 1980, and ASHRAE Handbook of Fundamentals 2017). The effective leakage area was calculated using the results of a blower door test (0.6 1/h at 50 Pa) performed after the house was fully constructed (Fanney et al. 2015, Ng et al. 2015). The monthly average infiltration rates modeled ranged from 0.03 1/h in summer to 0.07 1/h in winter, where the assumed volume included the basement, first, and second floors (not that the attic).

Internal Airflow

The fraction of airflow from heating, ventilating and air-conditioning (HVAC) system to each zone was determined from as-built drawings (Building Science Corporation 2009), where flow rates were spot-checked post-construction. The flow rates specified on the drawings at the registers for each zone were summed to calculate the fraction of flow supplied to each zone. To estimate the airflow between zones, a mass balance was performed on each zone during each time step.

Interior Thermal and Humidity Capacitance

ASHRAE Standard 90.2 (2007) provides an estimate of the internal capacitance of buildings, as shown in Equation (1). The NZERTF contains no furniture, therefore it is assumed that the mass of furniture and other contents is negligible, so the internal thermal mass is comprised only of the internal structural mass.

$$C_{zone,i} = \begin{cases} A_i c_g \left(24.41 \frac{kg}{m^2}\right) + V_i \rho_a c_{p,a}\,, & 1 \le i \le 3 \\ V_i \rho_a c_{p,a}\,, & i = 4 \end{cases} \quad (1)$$

where i is the zone number, $C_{zone,i}$ is the capacitance of each zone. A_i is the floor area of the zone, c_g is the heat capacity of gypsum board (1.09 kJ/(kg·K)), V_i is the volume of the zone, ρ_a is the density of air (1.204 kg/m^3), and $c_{p,a}$ is the heat capacity of air (1.005 kJ/(kg·K)).

The simulation model requires a humidity capacitance ratio to model the dynamic response of internal humidity. The humidity capacitance ratio is defined as the ratio of the mass of the water in the air contained in each zone and the mass of the water in other materials in the zone (e.g., the walls and furnishings) to the mass of the water in the air. The mass of water in other materials was estimated as the mass of water stored in the internal structure and calculated using the sorption isotherm for gypsum board at 40 % relative humidity. The mass of water in the air was calculated using an air temperature of 22 °C and a relative humidity of 40 %, i.e. 12.1 kg.

2.2 Model Boundary Conditions – Weather and Occupancy Schedules

The power for the plug loads, appliances, and lighting, the measured daily water draw volumes (which are included in the models of the DHW system and the latent load), and the average measured water mains temperatures were input to the model. Weather data measured on-site, which includes the outdoor dry-bulb temperature, outdoor wet-bulb temperature, irradiation on the plane of the solar panel array, and the measured water mains temperatures, were also input to the model. The other weather data inputs, which include the atmospheric pressure, wind direction and speed, and total sky cover, were collected at an airport located approximately 6.4 km away from the house. On-site ground temperature measurements were not available, so the ground temperatures at the basement walls and floor were predicted using model Type 1244 (TRNSYS 17 2013), which requires as inputs the soil properties, the deep earth temperature (14.2 °C), the amplitude of the soil surface temperature fluctuation over a year (7 °C, which yields a minimum of 7.2 °C and a maximum of 21.2 °C) , the day of the minimum soil surface temperature, and the basement dimensions.

2.3 Model Time Step

A time step of one minute was used because the equipment controls operate at approximately this time scale. For example, the heat pump triggers a higher stage of operation after running in the lower stage for 10 min, and the defrost cycle on the HRV causes the fan to run in recirculation mode for 7 min.

2.4 Original Subsystem Models

Heat Recovery Ventilator (HRV)

A heat recovery ventilator (HRV) was used to bring outdoor air into the NZERTF and was modeled using Type 667b for the heat exchanger and Type 111b for the two fans. This unit provides sensible heat exchange between the outdoor air supply and the exhaust air from the indoors. The lowest speed setting on the HRV, which provided 120 % of the minimum outdoor airflow specified by ASHRAE Standard 62.2-2010, was selected (Fanney, et al. 2015), which, according to the manufacturer's specifications, provides approximately 171 m^3/h of air. The sensible effectiveness specified by the manufacturer was reported under heating conditions only and varied with air speed. The coefficients for the correlation between the airflow and the effectiveness were determined from the data provided in the manufacturer's specifications, resulting in a sensible effectiveness of 0.75. The power consumption of the original HRV is also based on the airflow rate and was listed in the manufacturer specifications. The HRV runs continuously, but has a defrost mode during which it recirculates the indoor air.

Air-to-Air Heat Pump

The air-to-air heat pump in the NZERTF is a split-system heat pump with a two-step scroll compressor and a variable-speed air handler fan, modeled using Type 922. The heat pump is controlled by a thermostat, modeled using Type 974 and equation blocks. The heat pump has three heating stages, two cooling stages, and two dehumidification stages.

The heat pump operation is both temperature- and time-triggered, and the thermostat is located in the living room on the first floor of the NZERTF. The setpoints and deadbands are all adjustable within a range defined by the thermostat manufacturer. The various stages are triggered when the zone's temperature moves outside the deadband or the previous stage has been running longer than a specified time-out limit. In the third stage of heating, an electric resistance heater is energized. Dehumidification mode is activated if the humidity in the living room is greater than 50 % but the temperature setpoint is satisfied. The values for the

thermostat's specified setpoints, deadbands, and time-out limits are listed in Table 1, which is presented in "Thermostat setpoints and deadbands" within section 2.5.

The performance of the heat pump in first and second stage heating and cooling mode was modeled using manufacturer's data and the assumption that the coefficient of performance (COP) is the same for both stages. The capacity of the first stage is specified as 67 % of the capacity of the second stage for both heating and cooling modes. The model did not incorporate any cycling losses. Because the manufacturer's information did not specify the sensible heat ratio, the default sensible heat ratio of 0.77 was used. The first stage dehumidification mode was assumed to have the same capacity and power as first stage cooling mode, but a lower airflow rate. In second stage dehumidification mode the cooled, dehumidified air leaving the evaporator is reheated to the cooling setpoint by hot refrigerant that bypasses the condenser. The performance for this stage was calculated by assuming the cooling process occurs with the same total capacity and COP of first stage cooling mode, and the reheat occurs with no change to performance. To evaluate the performance of the heat pump at conditions different from the rated conditions, default performance maps from Type 922 were used. The program performance maps are external files consisting of data for the change in performance of the heat pump with respect to the rated performance given temperatures and airflow rates varying from the rated conditions.

Domestic Hot Water

The domestic hot water (DHW) system consists of a solar hot water (SHW) system and a heat pump water heater (HPWH) system. The SHW system preheats the water, which is then heated to the setpoint by the HPWH, if necessary, before going to its end use. A schematic of the system is shown in Figure 2.

The SHW system in use during the first year of operation uses a 303 L storage tank (modeled with Type 534), a cross-flow heat exchanger (Type 91), two pumps to circulate fluids through the heat exchanger (Type 114), and two single-glazed, flat plate solar collectors (Type 1b) with an aperture area of 2.1 m^2 per collector, facing south at an 18.4° tilt. The solar collector loop uses a 50 % by volume propylene glycol solution (brine). In addition to these components, the system piping and the heat loss from this piping is also modeled using Type 31. The parameters required to model the solar collectors were provided by the Solar Rating and Certification Corporation (Solar Rating & Certification Corporation, 2011). Seven nodes were used to model the stratification in the SHW storage tank. The tank dimensions and the location of inlets and outlets were

specified by the manufacturer. The loss coefficients were assumed to be the same as the loss coefficients for HPWH tank, discussed in the next section. A heat exchanger effectiveness of 0.8 was chosen based on expectations for a high performance solar hot water system (Duffie and Beckman 2013); no information about the effectiveness was available from the manufacturer. The brine and water pumps were modeled as single speed pumps using the manufacturer recommended flow rate and the corresponding power.

The HPWH system uses an integrated heat pump water heater and 189 L tank. After the water from the SHW tank passes through the tempering valve it enters the HPWH tank. The HPWH elevates the water temperature in the tank, if necessary, in order to maintain the setpoint.

The rated HPWH capacity, power, and airflow rate were provided by the manufacturer. The HPWH model (Type 938), like the air-to-air heat pump model, uses normalized performance data maps to interpolate the performance of the heat pump at conditions differing from the rated conditions. The manufacturer specified COP of the heat pump was 2.36, as evaluated using 2007 Department of Energy test procedures (DOE, 2007). The specified heating capacity of the heat pump was 1583 W when operating in high speed mode. The HPWH tank also has two 3800 W heating elements, modeled using Type 1226, although only the upper element was activated in the operating mode used during the first year of NZERTF operation. The HPWH tank is modeled using Type 534 and the dimensions and the inlet and outlet positions are specified by the manufacturer. The stratification of the tank was modeled using five nodes. The tank's skin loss coefficient, 0.59 W/(m^2·K), was estimated using the standby heat loss of the tank specified by the manufacturer. The deadbands for the heat pump (±4.2 K) and heating element (range from 16.8 K below setpoint up to the setpoint) temperature sensors, the fan power (5 W), and the standby power (7 W) were determined through correspondence with the manufacturer. After exiting the HPWH tank, the water flows through a manifold distribution system in the basement where it is directed through insulated tubing to the individual faucets, showerheads, or appliances. This manifold distribution system is simplified and modeled as two pipes: one directing hot water to the first floor end uses and the other to the second floor.

Photovoltaic System

The PV array is modeled using Type 194b, which used the 5-Parameter model presented in De Soto (2004). A tau-alpha product for normal incidence of 0.95 was assumed, and the extinction coefficient-thickness product of the cover default value of 0.008 was used.

The NZERTF uses thirty-two 320 W PV modules connected to a net energy meter, which allows surplus electricity to be exported to the grid. These modules are facing south at an angle of 18.4° and are arranged in four rows of eight. The maximum power of the modules at standard test conditions is 10.24 kW. Two inverters with an efficiency of 95.5 % are used to convert the direct current from the PV modules to 60 Hz alternating current.

2.5 Modified Subsystem Models

Although the NZERTF is a well-documented and carefully monitored and controlled facility, creating an accurate detailed model was challenging. The original model provided estimates of the thermal load or electricity consumption with discrepancies that need to be mitigated through model modification. A comprehensive analysis was conducted to identify the factors causing the deviation of each subsystem. In many cases the measured data were sufficient to estimate the actual performance of the equipment, which in some cases differed from the performance associated with the manufacturer's specifications.

To achieve a more accurate model of the NZERTF, many of the estimated parameters in the original model were updated using measured data after the first year of operation was complete. These changes led to a more accurate "modified" model that exhibited less discrepancy between the measured data and simulation results. The photovoltaic system in the original model predicted the energy generation well and did not need to be modified. All other subsystems were modified in some way, as discussed in this section.

Interior Thermal Capacitance

The capacitance of the floors, roof, and external walls are fixed by the properties library in the program, which was used when specifying the materials used in the construction of the NZERTF. However, the capacitance of the internal furnishings and the internal structural mass is a required parameter for each zone. This capacitance was estimated for the original model using ASHRAE Standard 90.2 (2007). The estimated interior thermal capacitance for the ground floor was 4317 kJ/K. For the modified model, the internal capacitance was adjusted until the dynamic first floor temperature response of the model matched the experimental measurements in the living room (thermostat location) for two periods of time (6 h and 7 h) when the heat pump was not running and there were no solar irradiation gains. The resulting modified interior thermal capacitance of the ground floor was 12000 kJ/K.

Heat Recovery Ventilator

To modify the HRV, parameters were adjusted in the program to reflect the measured values of these parameters. The average airflow rate was adjusted from 171 m^3/hr to 196 m^3/hr, the average power consumption was adjusted from 54 W to 63 W, and the average sensible effectiveness was adjusted from 0.75 to 0.72. The power and sensible effectiveness versus mass flow rate curves were adjusted accordingly. Furthermore, the HRV defrost cycle runtimes and temperature trigger were adjusted to reflect the observed behavior.

Air-to-Air Heat Pump Performance

The original heat pump model inaccurately simulates the physical heat pump because all of the information necessary for modeling each stage of the heat pump was not provided in the manufacturer specifications. Where information was provided, it was found that the physical heat pump does not perform exactly as the manufacturer specifications state in terms of both its capacity and power. To modify the heat pump, the rated capacity, power, airflow rate, and performance maps were revised using measured data. The performance maps for the heat pump were modified using heat pump performance versus outdoor dry bulb temperature provided by NIST (Leyde, 2014). The rated performance and airflow rate at each stage of heating, cooling, and dehumidification were then modified using minutely heat pump data provided by NIST. The standby energy observed from the measured data was also added to the simulation model.

Air-to-Air Heat Pump Defrost Cycle

One aspect of the heat pump operation that is neglected by the program type used to model the heat pump is the defrost cycle. During normal operation, frost may build up on the outdoor coil, reducing the heat pump's capacity and efficiency. To melt the frost from the coil, the heat pump operates in reverse to heat the outdoor coil and the supply air is heated with an electric resistance heater. This defrost cycle is activated after 90 min of accumulated compressor runtime if the outdoor temperature is below 1.7 °C. To include the defrost cycle in the modified model, the heat pump's measured electrical energy during defrost time periods was linearly correlated to the outdoor dry bulb temperature. This correlation was used in the program to predict the electrical energy used each time a defrost cycle was activated.

Thermostat Setpoints and Deadbands

To better predict the actual behavior of the NZERTF the heating mode setpoint, the dehumidification setpoint, and the heating mode, cooling mode, and dehumidification mode deadbands were adjusted in the program, as shown in Table 1. The proceeding three paragraphs discuss how the thermostat settings were adjusted.

There were a number of problems related to the thermostat in matching the model to the measurements. The thermostat is located in the living room, so the temperature and humidity measurements from the living room were used to study the thermostat control logic. While analyzing living room temperature data on a minute basis, it was noticed that the heating setpoint and both the heating and cooling deadbands did not match the values programmed into the thermostat. The heating setpoint was specified as 21.1 °C, yet the measured temperature in the living room appeared to be meeting a setpoint of approximately 20.5 °C. The deadband for first stage heating was specified as 0.56 °C, but the data showed the heat pump at times turning on after the temperature fell only 0.1 °C. Because the deadband used in the original simulation model is larger than what is observed in the data, the heat pump in the model stays on for periods of time that exceed the time-out limits, which triggers the second and sometimes the third stages of heating. These differences resulted in significant errors in predicted energy use between the original model and the observed data because of the lower efficiency exhibited by the higher stages.

The measured data during the cooling season did not show a noticeable discrepancy relative to the setpoint used in the original model. However, the measured deadband during cooling appeared to be approximately 0.2 °C, as opposed to the specified deadband of 1.1 °C in the original model. The measured data also show that the second stage dehumidification mode acted to keep the relative humidity between approximately 48 % and 50 %. The relative humidity deadband was not specified by the manufacturer and the dehumidification mode had been assumed to be triggered at a relative humidity of 51 % in the original simulation model.

Two other inconsistencies were noticed during cooling season operation. The first stage of the dehumidification mode is observed to last approximately 6 min rather than the specified 10 min. Also, it was observed that the second stage cooling does not consistently turn on after 40 min (as it should according to the thermostat program). Data for a time period in August showed the heat pump rarely switching to second stage even after more than 40 min of operation in first stage. However, minute data collected for a time period

in September showed the heat pump operating as-programmed; that is, it consistently switched to second stage after 40 min. This unpredictable behavior could not be replicated in the model.

It was also noted that the actual thermostat did not always follow the specified control logic, i.e., setpoints, deadbands, and run-times. These differences between the programmed logic and the actual behavior cause discrepancies in the predicted power, efficiency, and runtime of the heat pump, even in the modified model. Temperature measurements confirmed that the observed thermostat behavior was not attributed to temperature gradients in the living room or the wall where the thermostat is mounted. At this time the cause of the thermostat malfunction is unknown, but may be related to an internal fault in the thermostat's temperature measurement.

Domestic Hot Water

To modify the SHW system, the circulating pumps' power and flow rates, the heat exchanger effectiveness, and the solar hot water tank heat loss coefficient were adjusted in order to better match experimental data. The SHW tank heat loss coefficient was increased from 0.6 W/(m^2·K) to 1.0 W/(m^2·K) to achieve a better match between the predicted and measured water temperature leaving the solar hot water system. The SHW tank in the NZERTF was observed to behave as though it were fully mixed, so the number of nodes in the SHW tank was reduced from seven to one, which further improved the correlation between the predicted and measured water temperatures and volumes. The most significant change in the SHW system model was the heat exchanger effectiveness. The effectiveness of the heat exchanger was measured to be 0.44, which is a significant reduction relative to the effectiveness of 0.8 that was assumed in the original model.

The HPWH was modified using measured data for the heat pump and heating element in a way that is similar to how the air-source heat pump was modified. While the air-source heat pump was sufficiently instrumented to allow in-situ measurements to be used for this process, the HPWH was not and therefore results from tests performed by NIST on the same HPWH model (but a different physical piece of hardware) were used to modify the control logic and the COP. The modified capacity and COP of the heat pump at typical conditions (an ambient air temperature of 21.1 °C, a relative humidity of 50 %, and the temperature of the water entering the heat pump being 48.9 °C) was 1557 W and 2.02, respectively, relative to the original values of 1589 W and 2.21.

3 Results

Overall Heat Transfer Coefficient of the House

The overall heat transfer coefficient (UA) of the house (also known as the overall conductance) is computed as the slope of the line fit to the measurements of total thermal energy provided by the HVAC system each day versus the difference between the outdoor and indoor dry bulb temperature. Note that this is not a strict definition of UA since the HVAC load is not exclusively related to heat transfer through the envelope; the UA calculated here is also affected by airflow through the HRV, occupant and plug loads, and solar heat gains. The original model predicted a UA of 4.83 kW·h/(day·K) whereas the measured UA was 5.07 kW·h/(day·K). Modifying the model resulted in slightly better agreement between the predicted and measured UA, with modifying the HRV performance contributing the most to the change in UA (described below). The modified model's UA was 5.14 kW·h/(day·K).

HRV

The HRV introduces both sensible and latent loads to the house that must be met by the heat pump. Figure 3 shows the original and modified simulation latent and sensible loads introduced by the HRV compared to the measured loads. The measurement expanded uncertainty for a nominal operating condition is shown for the sensible (20 %) and latent loads (20 %) (Ng and Payne, 2016); these uncertainty values, and all others presented in the paper, are reported at the 95 % confidence interval (k = 2). The monthly loads introduced by the HRV in the original model are less than the loads introduced by the HRV in the modified model because the predicted average airflow rate in the original model was 12 % less than the measured average airflow rate.

Overall, the modified simulation model under-predicts the sensible load and over-predicts the latent load. The difference in the loads may be caused by measurement uncertainty and variation in the apparent sensible effectiveness and the airflow rate of the physical HRV, as well as small differences between the measured and predicted temperature and humidity ratio of the return air.

The original and modified simulation results and the measured annual energy consumption, average HRV effectiveness, and average flow rate are listed in Table 2. Also listed are the percent differences between the model's predicted values and the measured values.

Thermal Loads

Figure 4 compares the measured and predicted monthly integrated average thermal load met by the air-source heat pump. The original simulation model over-predicts the heating load by 11 % and under-predicts the cooling load by 15 %. The modified model over-predicts the heating load by 4 % and under-predicts the cooling load by 5 %. The remaining discrepancy in the thermal loads predicted by the modified model may be caused by a combination of factors including measurement error as well as inaccuracy of the model representations of infiltration, UA of the building, solar gains, and loads introduced by ventilation, equipment, appliances, plug loads, and occupants. The uncertainty of nominal cooling, 9 % (k = 2) and heating, 5 % (k = 2) operating conditions are overlaid for cooling- and heating-dominated months, respectively (Davis et al., 2014).

Air-to-Air Heat Pump

The electrical energy required to operate the air-to-air heat pump depends on the thermal load as well as the heat pump operating stage and the performance of the heat pump when operating in that stage. Table 3 and Figure 5 compare total heat pump electrical consumption measurements to the predictions from the original and modified simulation models, divided into the cooling/heating stages, defrost, and standby. Electrical power measurement expanded uncertainty (k = 2) is 2 % (Davis et al., 2014).

The original simulation model under-predicts the total electrical energy required in the cooling season by 32 %. In the heating season it predicts the total energy required to within 4 %. However, the original model over-predicted the energy used by the first and second stages of heating mode by 15 % and did not predict any of the 423 kWh of energy used by the heat pump for defrost cycles. These two discrepancies canceled out, resulting in a prediction of total heating season electrical energy that nearly matches the measurements.

Modifying the model decreased the percent difference in the total predicted cooling mode electrical energy with respect to the measured energy from -32 % (for the original model) to 13 % (for the modified model). The previously mentioned modified parameters, including the HRV airflow, the heat pump performance, and the smaller deadband, resulted in the increase of the electrical energy consumption. While the prediction of total cooling energy improved with the modified model, there is still a large discrepancy occurring in July primarily caused by the second stage dehumidification mode running more frequently in the model than it does in the actual NZERTF. The heat pump COP is relatively low in second stage

dehumidification mode (compared to the cooling modes) because the supply air is reheated, effectively reducing capacity. Over-predicting 2nd stage dehumidification in the model therefore resulted in significantly over-predicted energy use.

In heating, the modified model somewhat increased the percent difference between the predicted and measured total heat pump electrical energy from 4 % (for the original model) to 10 % (for the modified model). Although the original model's heating energy matched the measured data more closely, the modified model better matched the energy consumed by the first and second stages, defrost, and standby. The exception to the improved prediction with the modified model was the third stage resistance heater energy. The resistance heater ran less often in the modified model because the deadband was smaller, causing the heat pump to run for a shorter period of time and the third stage to be triggered less often.

The thermostat is a likely contributor to the discrepancy in the amount of time that the system spends in second stage dehumidification mode and third stage heating mode. Although the setpoints and deadbands were modified, the model does not reproduce the actual thermostat behavior consistently because the thermostat itself does not seem to operate consistently, as discussed in the "Thermostat Setpoints and Deadbands" section. Another contributor to the discrepancy between the measured data and program predictions is the assumption that each floor behaves as one zone. In reality, rooms on the same floor are often at slightly different temperatures and relative humidity. The humidifiers simulating the occupant latent load in the test facility are located in the kitchen, so the relative humidity is often higher in the kitchen than in the living room. However, because the entire first floor is modeled as a single zone in the program, the added moisture impacts the relative humidity throughout the floor equally. The humidity measurement at the thermostat will subsequently be higher in the model, which could increase the frequency of the activation of heat pump second stage dehumidification. Thirdly, the airflow between each floor in the program may not be the same as the airflow within the actual NZERTF. A final consideration is that the uncertainty of loads introduced by the HRV is rather large (>25 %), so these modeled-introduced loads may differ somewhat from the actual introduced loads, contributing to the discrepancy in the second stage dehumidification mode and third stage heat pump mode.

SHW System

The temperature of the DHW is recorded at various location in the NZERTF every three seconds with an expanded uncertainty (k = 2) of 0.2 °C. Figure 6 compares the measured and predicted SHW monthly integrated average temperatures of the water entering and exiting the SHW tank, calculated only for the periods the water is flowing. Table 4 compares the program-predicted to the measured energy delivered by the SHW system, as well as the electrical energy consumed by the SHW pumps.

The primary reason that the original model under-predicts the volume of hot water delivered by the SHW system is that the model over-predicts the SHW outlet temperature for much of the year. Therefore, the water in the model requires more tempering as it exits the SHW system and less hot water is drawn from the system. The volume of water delivered by the NZERTF SHW system was further increased by the tempering valve not being operational from July 1 through September 26, 2013.

The dip in the temperature of the water exiting the SHW tank occurring in August was caused by the SHW system pumps not being operational from August 24, 2013 through September 3, 2013, which resulted in the water in the solar tank not being heated by the solar collectors before it is drawn into the HPWH tank. Also, from July 1 through September 26, 2013, the length of pipe between the tempering valve and the HPWH tank was 7.2 m and the tempering valve did not operate. After September 26, the length of pipe was shortened to 2.2 m and the tempering valve controlled the entering water temperature to the setpoint. These tempering valve, pump operation, and pipe length changes were made in the modified model.

Incorporating these changes to the model and modifying the SHW system resulted in decreasing the absolute value of the percent error between the predicted and measured pump energy consumption from 30 % to 4 %. Figure 6 shows that the average monthly water temperatures match the measured results more closely, and Table 4 shows that average monthly water volume and the monthly SHW loads predicted by the modified model agree more closely with the measured data as well.

HPWH System

The temperature of the water exiting the SHW tank during the summer months predicted by the original simulation model was higher than what was measured, so the temperature of the water entering the HPWH tank is higher as well. The original simulation model under-predicts the temperature of the water exiting the HPWH tanks during the summer months because it operates less frequently, allowing the water to cool to a temperature nearer to the heat pump's lower deadband.

The original simulation model under-predicts the amount of energy supplied by the HPWH system by 33 %. This discrepancy occurs because simulation over-predicts the temperature of the water exiting the SHW system and under-predicts the temperature of the water exiting the HPWH tank. The discrepancy is also caused by the volume of water delivered by the HPWH system being under-predicted, largely because of the under-prediction of the volume of water delivered by the SHW system. The electrical consumption predicted by simulation is 46 % less than the measured electrical consumption, which can largely be attributed to the under-prediction of the thermal load. Another contributing factor to the energy consumption discrepancy is the lack of resistance heat predicted by the original simulation model. The HPWH electric heating element was active in the NZERTF every month except for June 2014 and July 2013, but the node containing the heating element never reached a temperature that is low enough to trigger the heating element in the original simulation model. Note that from November 25, 2013 through December 5, 2013, the heat pump was not operational; therefore, during that time period only the heating element was used to heat the water in the HPWH system. Therefore, the measured heating element energy is greatest in November and December, as seen in Table 5.

The improved prediction of SHW outlet temperatures in the modified model resulted in better prediction of the HPWH inlet temperatures, as shown in Figure 7. The measurement expanded uncertainties (k = 2) for the temperatures in Figure 7 are 0.2 °C. Incorporating the heat pump 11 day down-time into the modified model and modifying the HPWH model caused significant improvement in the comparison between the predicted and measured HPWH tank outlet temperature, annual HPHW energy delivered, and energy consumption. However, as with the original model, the heating element was never triggered in the modified model except for the period of time that the heat pump itself was not operational. Because the program inlet and outlet temperatures, the hot water volumes, and the HPWH loads agree closely with the measured values, the cause of the discrepancy in heating element energy may be that the physical heating element is actually triggered at a higher temperature than specified by the manufacturer. Table 5 compares the monthly energy delivered and energy consumed by the HPHW system.

Both the total volume of hot water delivered and the total annual energy delivered by the DHW system predicted by the modified and original models match the measured data closely. The annual energy delivered by the DHW system is under-predicted by 6 % in the original model and by 5 % in the modified model. The

total volume of hot water delivered by the DHW system from September 2013 through June 2014 is under-predicted by 5 % in the original model and by 6 % in the modified model. For greater detail on the DHW simulation results, see Balke (2015).

Photovoltaic System

Snow covered at least part of the photovoltaic array on 38 days during the first year of NZERTF operation, limiting the array's energy production. The snow cover is partially accounted for in the simulation model because the solar irradiation measured at the NZERTF is used in the model. On days of snow accumulation, less solar irradiation was recorded because the pyranometer was also covered with snow. However, the snow tended to melt off the pyranometer before the PV array was uncovered. Therefore, on days following heavy snowfall the pyranometer often recorded solar irradiation while the PV array remained covered in snow.

Figure 8 compares the predicted energy generated by the PV system (AC power to the house) to the measured energy generated. PV generation measurement expanded uncertainty (k = 2) is 1.0 % (Davis et al., 2014). Also shown in Figure 8 for reference is the total solar insolation measured at the NZERTF each month. Six days of power generation measurements in August were not recorded. These six days were deleted from the predicted results to better compare with the recorded data. As mentioned previously, the PV system was not modified, so the original and modified models' results are identical.

Overall, the annual PV energy generated predicted by the simulation models agrees with the measured PV energy generated to within 3.1 %. The average absolute value of the percent error in the monthly totals is 6.6 %. The largest percent errors occur in February, March, and December, which are also the months with the greatest number of days during which snow covered at least part of the PV array.

4 Conclusion

The original simulation model predicted an annual energy consumption of 13.8 % less than what was measured. The simulation model (both modified and original) predicted an annual PV generation 3.1 % more than measured. The original model therefore predicted 2697 kW·h of surplus energy. Modifying the model resulted in a reduction in the difference between the predicted and measured total annual energy consumption as well as in the difference for each subsystem. The absolute value of the percent difference between the

predicted and measured annual energy consumed was reduced to 1.6 % for the modified model. Table 6 shows the predicted and measured annual electrical energy generation and consumption as well as the annual consumption for each subsystem. For more information on the total electrical generation and consumption, refer to Balke (2015).

The lack of actual occupants in the NZERTF, the regularly scheduled plug load activation and water draws, and the careful monitoring of the NZERTF make it both an unusual and ideal situation for comparing modeled results with physical residential house behavior. The NZERTF's occupancy, plug, appliance, and lighting loads, and water draws were carefully controlled, and the model developed to simulate the NZERTF is detailed. Even so, the simulation model developed using information that was available before the NZERTF's first year of operation was not able to accurately predict some aspects of the residence operation. This type of original building model is more typical, and is used at the design stage to predict loads and electrical consumption. Modifying the model decreased most of the differences between the predicted and measured results. However, discrepancies persisted between the results of the modified model and the measurements of the air-source heat pump's dehumidification mode and auxiliary heating mode, and the HPHW system's heating element use. Precisely modeling even a highly controlled, accurately measured facility is still challenging.

There remains a significant discrepancy between the predicted and measured electrical energy associated with the heat pump's third stage resistive heater and second stage dehumidification mode. These discrepancies are largely driven by differences in the gradient and dynamic behavior of temperature and humidity in the house; with time-triggered activation of higher heat pump stages these differences significantly impact the time spent in each stage and therefore overall energy usage. Therefore, to make the model more accurate, the house model can be further subdivided into more zones, and a better model of the infiltration and the movement of air between zones can be included; this could be accomplished, for example, using airflow program (Dols and Polidoro, 2015, Dols et al. 2015a and 2015b). Furthermore, a thermostat that consistently applies the control logic should be used in the NZERTF to resolve the issues discussed in the "Thermostat Setpoints and Deadbands" section.

A number of interesting simulations may now be performed using the modified model of the NZERTF in order to gain a deeper understanding of operation, applicability, and optimal design of net-zero energy

houses. For example, the simulations can be run using weather data from different climates to determine how well the house performs at various geographic locations. The house orientation, size, geometry, and number of windows, etc. can be varied in order to study the impact that these parameters have on the energy performance of the house, including its ability to meet a net-zero goal. The occupancy, hot water load, plug loads, and appliance schedule can also be varied to find how well the house performs when occupied by a family that deviates from the assumed family behavior.

Changes to the equipment within the house are particularly interesting and can also be investigated with the model. One of the most interesting and promising areas of investigation is the control strategy used for the heat pump. Different deadbands, setpoints, or time-triggers can be compared to the current control strategy. More advanced control strategies can be studied such as those that actively learn how to maintain comfort while minimizing the amount of time that the higher heat pump stages are used (which have lower efficiencies).

Finally, alternative equipment configurations can be examined. A ground-source heat pump using various ground source heat exchangers (vertical, horizontal and slinky) can be compared to the air-source heat pump used in the results presented here. Other ventilation systems, such as an enthalpy exchanger or simple mechanical ventilation can be compared to the HRV currently in place. Various DHW system configurations and tank sizes can be compared with the system used in the NZERTF during the first year of operation.

5 Acknowledgements

Part of this work was carried out at the University of Wisconsin - Madison with support by the National Institute of Standards and Technology under Grant 60NANB14D318_0 CD-450 and Award 60NANB14D318. Thanks is given to Doug Reindl and Lisa Ng for their careful review of the paper. Furthermore, the editing work of Wei Wu is gratefully acknowledged.

6 References

References

ASHRAE. 2017. ASHRAE Handbook of Fundamentals, Chapter 16 “Ventilation and Infiltration”. Atlanta: American Society of Heating, Refrigerating and Air-conditioning Engineers, Inc.

ASHRAE. 2007. ASHRAE Standard 90.2-2007. Atlanta: American Society of Heating, Refrigerating and Air-conditioning Engineers, Inc.

Balke, E. Modeling, Validation, and Evaluation of the NIST Net Zero Energy Residential Test Facility. Master’s Thesis. University of Wisconsin, Madison. 2016.

Building Science Corporation. 2009. National Institute of Standards and Technology Net Zero Energy Residential Test Facility As Built Architectural Plans. Somerville, MA: Building Science Corporation. <http://www.nist.gov/el/nzertf/>

Davis, M., W. Healy, M. Boyd, L. Ng, V. Payne, H. Skye, and T. Ullah. 2014. Monitoring Techniques for the Net-Zero Energy Residential Test Facility. NIST Technical Note 1854. <http://www.nist.gov/el/nzertf/publications.cfm>

De Soto, W. 2004. Improvement and Validation of a Model for Photovoltaic Array Performance. Master’s Thesis. University of Wisconsin, Madison.

DOE, 2007. 2007-10-22 Energy Conservation Program for Consumer Products: Test Procedure for Residential Central Air Conditioners and Heat Pumps; Final rule (EE-RM/RP-02-002), 10 CFR Part 430, FR 59906 , Oct. 22 (2007). Accessed from https://www.gpo.gov/fdsys/granule/FR-2007-10-22/07-5142.

Dols, W. S. and B. J. Polidoro (2015). CONTAM User Guide and Program Documentation. NIST Technical Note 1887. Gaithersburg, MD, National Institute of Standards and Technology.

Dols, W. S., L. Wang, S. J. Emmerich and B. J. Polidoro (2015a). "Development and Application of an Updated Whole-building Coupled Thermal, Airflow and Contaminant Transport Simulation Program (TRNSYS/CONTAM)." Journal of Building Performance Simulation 8(5): 326-337.

Dols, W. S., S. J. Emmerich and B. J. Polidoro (2015b). "Using coupled energy, airflow and indoor air quality software (TRNSYS/CONTAM) to evaluate building ventilation strategies." Building Services Engineering Research and Technology.

Duffie, J. A. and W. A. Beckman. 2013. Solar Engineering of Thermal Processes. Fourth Ed. Hoboken, NJ: John Wiley & Sons, Inc. p. 425.

Fanney, A. H., V. Payne, L. Ng, M. Boyd, F. Omar, M. Davis, H. Skye, B. Dougherty, B. Polidoro. W. Healy, and B. Pettit, 2015. Net-Zero and Beyond! Design and Performance of NIST’s Net-Zero Energy Residential Test Facility, Energy and Buildings, Vol. 101.

Hendron, R. and C. Engebrecht. 2010. Building America House Simulation Protocols, National Renewable Energy Laboratory, Building Technologies Program, U.S. Department of Energy.

Leyde, B. TRNSYS Modeling of the NIST Net Zero Energy Residential Test Facility. Master’s Thesis. University of Wisconsin, Madison. 2014. p. 12-13; 114-120.

"Net-Zero Energy Residential Test Facility (NZERTF) Homepage." NIST: Engineering Laboratory. NIST, 11 Sept. 2015. Web.

Ng, L. C. and W. V. Payne. Energy Use Consequences of Ventilating a Net-Zero Energy House. Applied Thermal Engineering, v 96, p 151-160, March 5, 2016, ISSN: 13594311; DOI: 10.1016/j.applthermaleng.2015.10.100

Ng, L., Persily, A. and Emmerich, S. 2015. Infiltration and Ventilation in a Very Tight, High Performance Home. 36th AIVC Conference Effective Ventilation in High Performance Buildings. Madrid, Spain: Air Infiltration and Ventilation Centre: 719-726.Omar, F. and S. T. Bushby. 2013. Simulating Occupancy in the NIST Net-Zero Energy Residential Test Facility. NIST Technical Note 1817. <http://www.nist.gov/el/nzertf/publications.cfm>.

NRCS, 2017. Natural Resources Conservation Service for soil temperature data Powder Mill Report Generator, National Water and Climate Center, NRCS, US Dept. of Agriculture. Web < https://www.wcc.nrcs.usda.gov/>

Sherman, M.H. and Grimsrud, D.T. 1980. Infiltration-pressurization correlation: Simplified physical modeling. ASHRAE Transactions 86(2):778. Paper DV-80-09-3

“Solar Collector Certification and Rating Sheet: Heliodyne, Inc. GOBI 406 001.” Solar Rating & Certification Corporation. Mar. 2011.

Torcellini, P., S. Pless, M. Deru, and D. Crawley. "Zero Energy Buildings: A Critical Look at the Definition." ACEEE Summer Study (2006): n. pag. Web. <http://www.nrel.gov/docs/fy06osti/39833.pdf>.

TRNSYS 17, A TRaNsient SYstems Simulation Program. 2013. TRNSYS. Solar Energy Laboratory, <http://sel.me.wisc.edu/trnsys/>.

(a) (b)

Figure 1. (a) CAD model of NZERTF used in simulation (Leyde 2014) (b) Photograph of the NZERTF ("Net-Zero Energy Residential Test Facility Homepage")

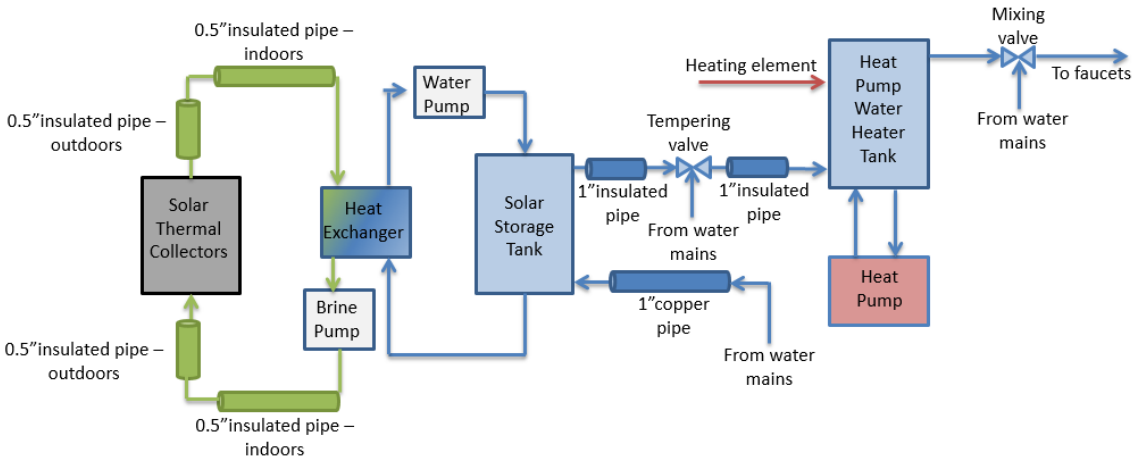

Figure 2. Schematic of the DHW system.

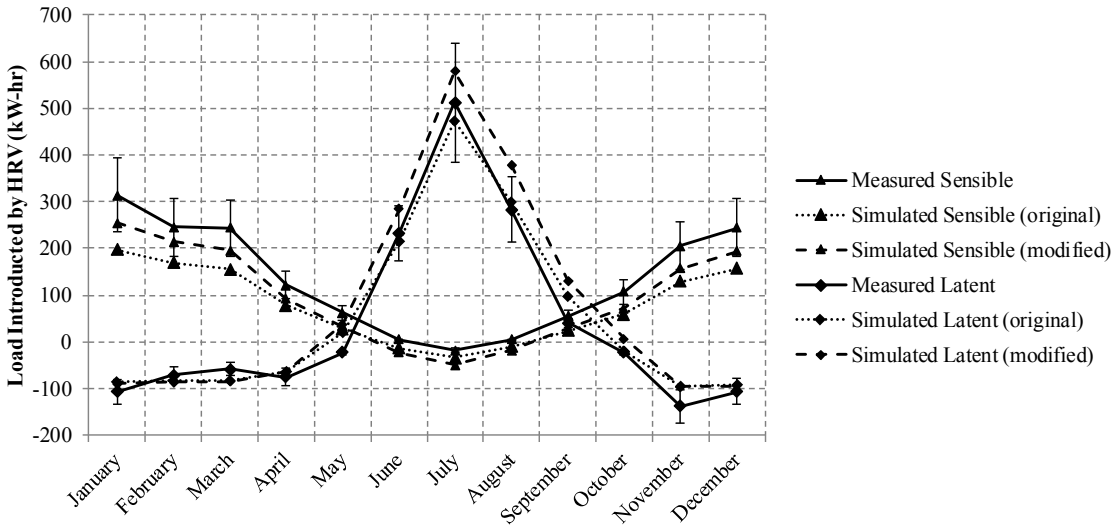

Figure 3. Measured vs. simulated monthly loads introduced by HRV.

Figure 4. Measured vs. simulated thermal energy.

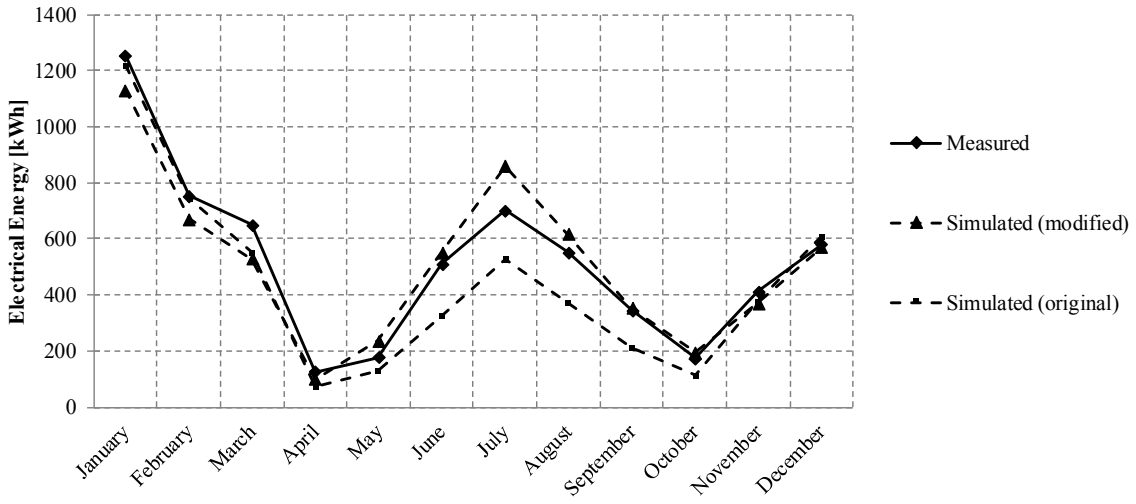

(a)

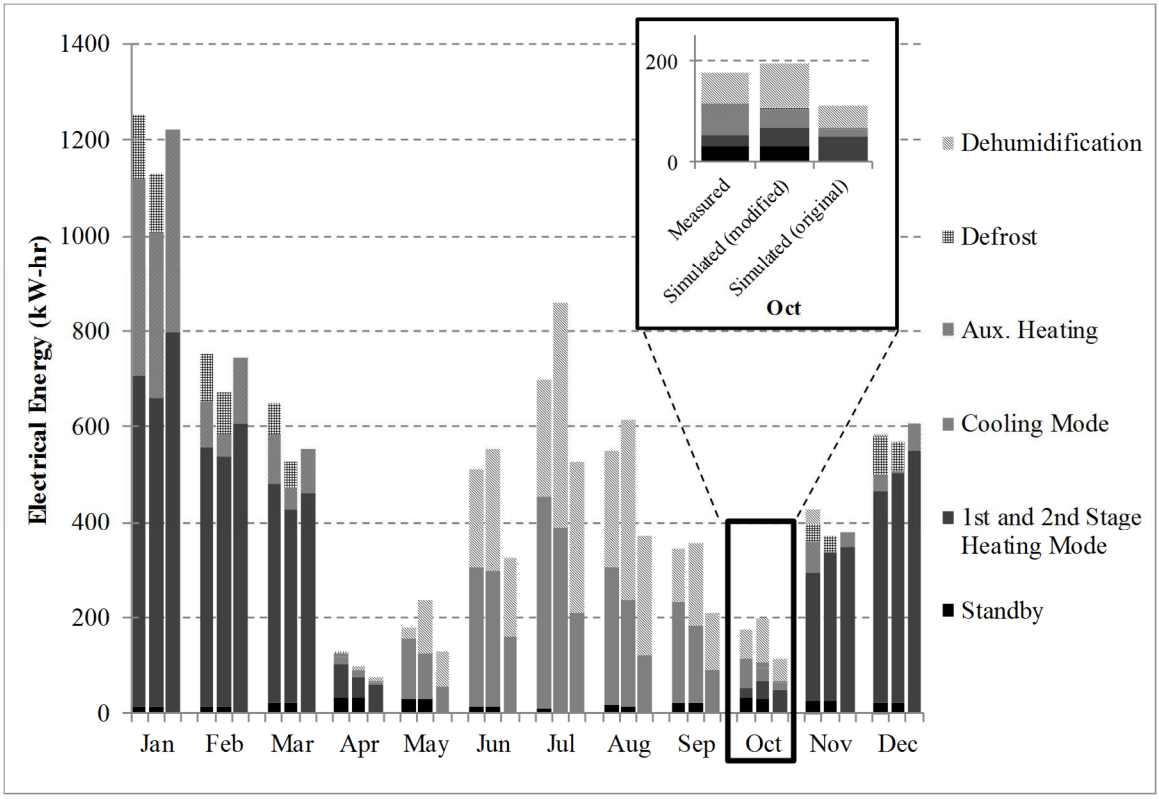

(b)

Figure 5. (a) Measured vs. simulated heat pump total monthly electrical energy. (b) Measured vs. simulated heat pump monthly electrical energy analysis.

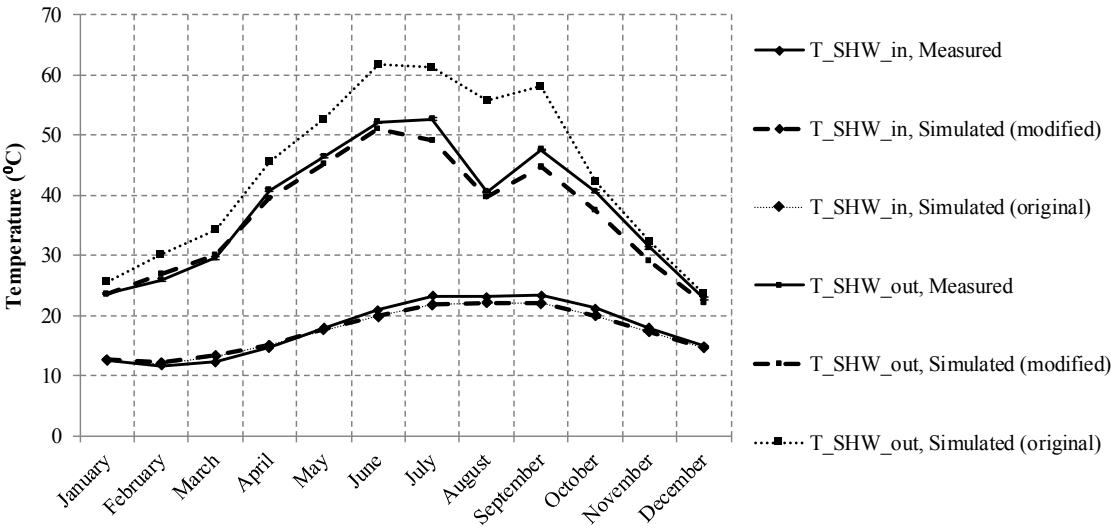

Figure 6. Measured vs. simulated SHW temperatures.

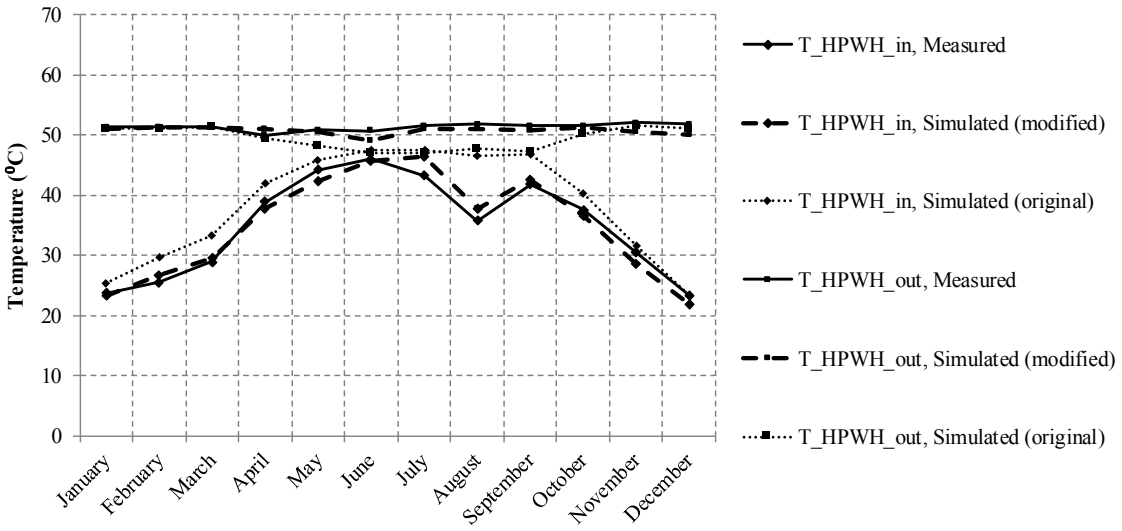

Figure 7. Measured vs. simulated predicted HPWH temperatures.

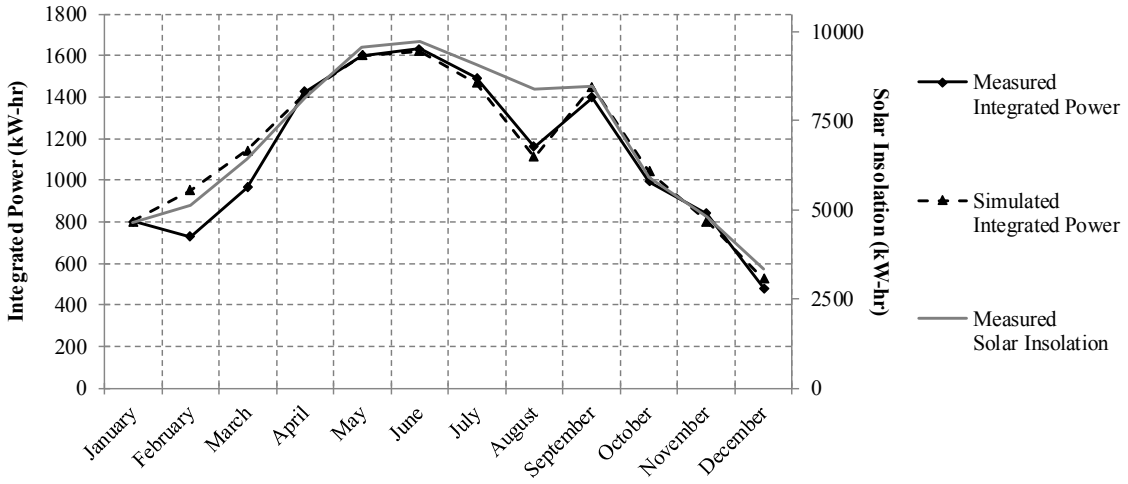

Figure 8. Measured vs. simulated PV power and solar insolation.

Table 1. Air-to-air heat pump control logic.

Mode	Setpoint		*Turn-on Trigger*						
				First Stage		Second Stage		Third Stage	
	Original	*Modified*		*Original*	*Modified*	*Original*	*Modified*	*Original*	*Modified*
Heating	21.1 °C	20.5 °C	Deadband (°C)	0.56	0.1	1.1	1.1	3.3	3.3
			Time Delay (min)	N/A	N/A	10	10	40	40
Cooling	23.9 °C	23.9 °C	Deadband (°C)	1.1	0.2	2.8	2.8	N/A	N/A
			Time Delay (min)	N/A	N/A	40	40	N/A	N/A
Dehumid.	50 %	48 %	Deadband (%)	1	2	N/A	N/A	N/A	N/A
			Time Delay (min)	N/A	N/A	10	6	N/A	N/A

* The original values are the setpoints, deadbands, and time delays programmed in the thermostat. The modified model values are the estimated observed values, but these values are not necessarily consistently followed.

Table 2. HRV Annual Performance Data

	Energy Consumption [kW · h]	Effectiveness [--]	Average Flow Rate [m^3/h]
Measured[1]	514	0.72	195
Simulated (original)	355	0.75	171
Percent Difference	*-31 %*	*4 %*	*-12 %*
Simulated (modified)	524	0.71	196
Percent Difference	*2 %*	*-1 %*	*1 %*

[1] *Measurement uncertainty is 1.9 % (at k = 2, 95 % confidence interval), (Davis et al., 2014)*

Table 3. Measured vs. simulated Heat Pump Annual Electrical Energy Analysis.

	Measured[1] [kW·h]	Simulated (original) [kW·h]	*Percent Difference (original)*	Simulated (modified) [kW·h]	*Percent Difference (modified)*
1st and 2nd Stage Heating	2496	2881	*15 %*	2442	*-2 %*
Auxiliary Heating (3rd Stage)	735	746	*2 %*	463	*-37 %*
Defrost	423	0	*-100 %*	361	*-15 %*
Cooling	1404	653	*-53 %*	1176	*-16 %*
Dehumidification	922	978	*6 %*	1486	*61 %*
Standby	262	0	*-100 %*	256	*-2 %*
Total Heating	3783	3627	*-4 %*	3404	*-10 %*
Total Cooling	2458	1631	*-32 %*	2780	*13 %*
Total Electrical Energy	6241	5258	*-15 %*	6183	*-1 %*

[1] *Measurement uncertainty is 1.9 % (at k = 2, 95 % confidence interval), (Davis et al., 2014)*

Table 4. SHW Performance.

	Energy delivered by SHW system					SHW Pump Energy Consumption					*SHW Water Delivered*				
Month	Measured[1] [kWh]	Simulated (original) [kWh]	*Percent Difference (original)*	Simulated (modified) [kWh]	*Percent Difference (modified)*	Measured[2] [kWh]	Simulated (original) [kWh]	*Percent Difference (original)*	Simulated (modified) [kWh]	*Percent Difference (modified)*	Measured[3] [L]	Simulated (original) [L]	*Percent Difference (original)*	Simulated (modified) [L]	*Percent Difference (modified)*
Jan-14	102	121	*19 %*	99	*-2 %*	20.4	12.5	*-39 %*	18.8	*-8 %*	7722	7368	*-5 %*	7323	*-5 %*
Feb-14	124	150	*21 %*	118	*-5 %*	19.8	13.9	*-30 %*	20.8	*5 %*	7113	6694	*-6 %*	6587	*-7 %*
Mar-14	158	186	*18 %*	146	*-8 %*	22.6	16.8	*-25 %*	25.4	*12 %*	7430	7318	*-2 %*	7240	*-3 %*
Apr-14	227	247	*9 %*	194	*-14 %*	29.0	20.7	*-29 %*	31.1	*7 %*	7118	6835	*-4 %*	6832	*-4 %*
May-14	237	263	*11 %*	215	*-9 %*	34.3	25.1	*-27 %*	37.6	*10 %*	7169	6533	*-9 %*	6869	*-4 %*
Jun-14	239	250	*4 %*	223	*-7 %*	34.8	25.0	*-28 %*	38.2	*10 %*	6634	5318	*-20 %*	6420	*-3 %*
Jul-13	239	231	*-3 %*	215	*-10 %*	35.7	23.8	*-33 %*	38.4	*7 %*	6710	5281	*-21 %*	6795	*1 %*
Aug-13	131	217	*65 %*	138	*6 %*	27.1	22.8	*-16 %*	26.5	*-2 %*	6833	5815	*-15 %*	6788	*-1 %*
Sep-13	204	218	*7 %*	176	*-14 %*	31.4	21.8	*-31 %*	30.9	*-1 %*	7794	5375	*-31 %*	6662	*-15 %*
Oct-13	173	173	*0 %*	138	*-20 %*	24.2	16.9	*-30 %*	26.3	*9 %*	8140	6702	*-18 %*	6885	*-15 %*
Nov-13	117	118	*1 %*	94	*-19 %*	22.0	13.3	*-39 %*	20.7	*-6 %*	7637	6636	*-13 %*	6953	*-9 %*
Dec-13	78	82	*5 %*	67	*-14 %*	18.2	10.0	*-45 %*	16.8	*-8 %*	7790	7231	*-7 %*	7415	*-5 %*
Total	**2029**	**2254.2**	***11 %***	**1825**	***-10 %***	**319.5**	**222.8**	***-30 %***	**331.4**	***4 %***	**74546**	**77106**	***-12 %***	**69185**	***-7 %***

** Measurement uncertainty at k = 2, 95 % confidence interval is: [1]3.4 %, [2]4.4 %, and [3]3.4 %, (Davis et al., 2014)*

Table 5. HPWH Performance.

	Energy delivered by HPWH					Total Electrical Energy Used by HPWH					HPWH Heating Element Electrical Energy Used				
Month	Measured[1] [kW·h]	Simulated (original) [kW·h]	*Percent Difference (original)*	Simulated (modified) [kW·h]	*Percent Difference (original)*	Measured[2] [kW·h]	Simulated (original) [kW·h]	*Percent Difference (original)*	Simulated (modified) [kW·h]	*Percent Difference (modified)*	Measured[2] [kW·h]	Simulated (original) [kW·h]	*Percent Difference (original)*	Simulated (modified) [kW·h]	*Percent Difference (modified)*
Jan-14	240.2	220.1	*-8 %*	234.6	*-2 %*	142.8	111.6	*-22 %*	133.3	*-7 %*	13.9	0.0	*-100 %*	1.5	*-89 %*
Feb-14	207.7	165.0	*-21 %*	188.1	*-9 %*	125.0	86.0	*-31 %*	109.2	*-13 %*	14.2	0.0	*-100 %*	0.0	*-100 %*
Mar-14	187.3	149.4	*-20 %*	182.7	*-2 %*	120.7	81.4	*-33 %*	109.6	*-9 %*	12.8	0.0	*-100 %*	0.0	*-100 %*
Apr-14	84.4	54.4	*-36 %*	105.2	*25 %*	72.7	35.3	*-52 %*	69.3	*-5 %*	3.3	0.0	*-100 %*	0.0	*-100 %*
May-14	54.7	16.1	*-71 %*	66.5	*22 %*	55.2	18.0	*-67 %*	51.2	*-7 %*	0.6	0.0	*-100 %*	0.0	*-100 %*
Jun-14	35.3	-8.1	*-123 %*	24.4	*-31 %*	46.1	5.5	*-88 %*	28.2	*-39 %*	0.0	0.0	*0 %*	0.0	*0 %*
Jul-13	42.1	-8.3	*-120 %*	30.4	*-28 %*	53.3	5.9	*-89 %*	32.2	*-40 %*	0.0	0.0	*0 %*	0.0	*0 %*
Aug-13	107.9	3.8	*-97 %*	100.3	*-7 %*	70.8	11.7	*-83 %*	65.9	*-7 %*	5.8	0.0	*-100 %*	0.0	*-100 %*
Sep-13	68.3	-3.3	*-105 %*	58.0	*-15 %*	57.0	8.4	*-85 %*	45.2	*-21 %*	3.2	0.0	*-100 %*	0.0	*-100 %*
Oct-13	118.7	73.8	*-38 %*	117.0	*-1 %*	82.5	44.1	*-47 %*	75.7	*-8 %*	3.2	0.0	*-100 %*	0.0	*-100 %*
Nov-13	172.0	151.1	*-12 %*	174.1	*1 %*	129.8	80.7	*-38 %*	122.4	*-6 %*	44.3	0.0	*-100 %*	40.1	*-10 %*
Dec-13	244.0	232.0	*-5 %*	238.8	*-2 %*	156.3	115.3	*-26 %*	148.3	*-5 %*	36.1	0.0	*-100 %*	33.8	*-6 %*
Total	**1562.6**	**1045.9**	***-33 %***	**1520.0**	***-3 %***	**1112.2**	**603.8**	***-46 %***	**990.5**	***-11 %***	**137.4**	**0.0**	***-100 %***	**75.4**	***-45 %***

** Measurement uncertainty at k = 2, 95 % confidence interval is: [1]3.4 %, [2]2.6 %, (Davis et al., 2014)*

Table 6. Measured and Predicted Annual Electrical Energy Generation and Consumption.

	Measured (kW·h)	**Simulated (original) (kW·h)**	***Percent Difference***	**Simulated (modified) (kW·h)**	***Percent Difference***
Lighting[1]	435	442	*1.4%*	442	*1.4 %*
Plug Loads[1]	2440	2462	*0.9%*	2462	*0.9 %*
Appliances[1]	1867	1898	*1.6%*	1898	*1.6 %*
Air-to-Air Heat Pump[1]	6241	5258	*-15.7%*	6184	*-0.9 %*
HRV[1]	514	355	*-31.1%*	524	*1.8 %*
DHW[1]	1432	827	*-42.3%*	1322	*-7.7 %*
Total Consumed[1]	13039	11241	*-13.8%*	12831	*-1.6 %*
PV[2]	13523	13937	*3.1%*	13937	*3.1 %*
Net Generation	484	2697		1106	

** Measurement uncertainty at k = 2, 95 % confidence interval is: [1]1.9 %, [2]1.0 %, (Davis et al., 2014)*